Experimental Study on Detonation Wave Initiation by Reflected Blast Wave in Laser Ignition

Tomoyuki Sato, Ken Matsuoka, Akira Kawasaki,
Noboru Itouyama, Hiroaki Watanabe, and Jiro Kasahara
Department of Aerospace Engineering, Nagoya University
Furo-cho, Chikusa-ku, Nagoya, Aichi, Japan

1 Background

Detonation is a supersonic combustion phenomenon [1, 2] that propagates in combustible mixtures at 2 ~ 3 km/s, and Pulse Detonation Cycle (PDC) is a kind of thermodynamic cycle that generates detonation waves intermittently [3]. Since PDC can generate jets and shock waves at high efficiency in a short and simple combustor, it is expected to be applied for high-accuracy Reaction Control Systems of rockets and small satellites, pre-detonators for small Rotating Detonation Engines, gas turbine engines, heat sprayers, and medical fields [4]. Generally, detonation waves are generated through Deflagration-to-Detonation Transition (DDT) process in PDC where an initial flame kernel develops into a detonation wave [5]. Therefore, the shorter time and length of DDT can contribute to realizing a more actively controllable detonation combustor. Direct ignition, instead of DDT, seems to be suitable for quick and short-distant detonation initiation, however, direct ignition requires a hundred to a thousand times of ignition energy for successful initiation [6, 7]. Therefore, this study focuses on the blast wave caused by laser emission as a new method to initiate detonations with such a small amount of energy as DDT and in such a short distance as direct ignition. Because it is possible to make a high temperature/pressure region by reflecting or focusing the blast wave by a wall or in a cavity, detonations can be initiated after the reflection. Hence, in this study, a laser beam was emitted vertically and horizontally toward the reflection wall and in an elliptical cavity to visualize the generation, development, and reflection of the blast wave so that the maximum pressure profile of the flowfield was estimated to compare with the strong/mild ignition limit proposed by Meyer and Oppenheim [8].

2 Equipment and Experiment Conditions

Figure 1 shows the cross-section of the combustor. The combustor has a cylindrical room that is filled with the combustible mixture and has a stage to put a vertical or a horizontal reflection wall and an elliptic cavity. The laser beam comes from the left in the figure and focuses in front of the wall or the cavity. Table 1 shows the experimental condition. In the experiments, a static, pre-mixed, stoichiometric ethylene–oxygen mixture was used, and an Nd: YAG laser beam was emitted toward the mixture. In the case of vertical and horizontal walls, the distance from the focal point to the reflection wall was varied. The experiment was recorded by a high-speed camera at 200 ns/frame with a 20 ns exposure time.

Correspondence to: sato@prop2.nuae.nagoya-u.ac.jp

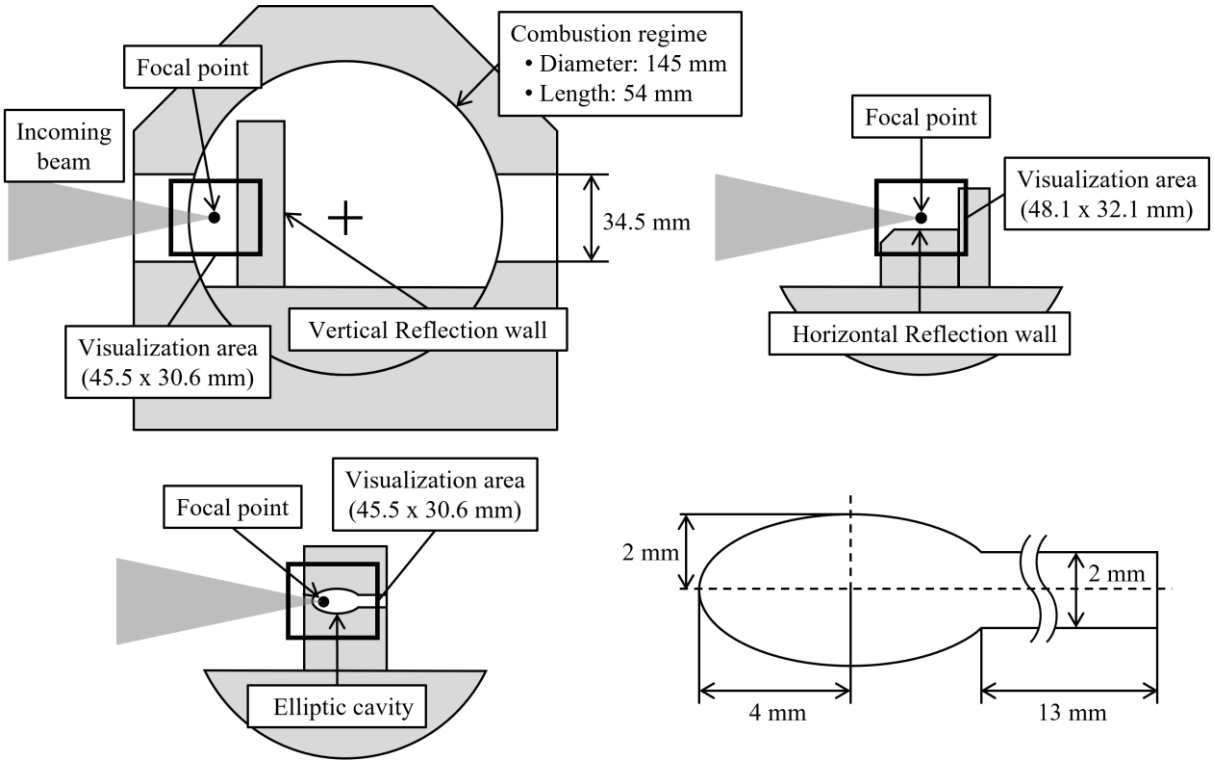

Figure 1: Cross-section of the combustor using vertical reflection wall (top left), horizontal reflection wall (top right), elliptic cavity (bottom left), and the configuration of the cavity (bottom right).

Table 1: Experimental condition

Gas	$C_2H_4 - O_2$ (stoichiometric)								
Initial pressure [kPa]	100				100				103
Laser	Nd: YAG laser, 1064 nm								
Emission time [ns]	5.0 ± 0.3								
Input diameter [mm]	25								
Focal length [mm]	200								
Emission energy, E [mJ]	200				200				36.1
Wall type	Vertical				Horizontal				Ellipsoid
Focal point – wall distance, L [mm]	2.06	2.86	2.98	3.66	1.41	1.54	2.44	3.09	-
Frame rate (ns/frame)	200								
Exposure time [ns]	20								

3 Results and Discussions

3.1 Laser ignitions using a vertical and a horizontal reflection walls

Figure 2 shows the successive schlieren images and their sketches in the case of a vertical reflection wall where the distance from the focal point to the wall was 3.66 mm. The generation and expansion of a spherical flame kernel and a blast wave were observed at t = 2 μs, and blast wave

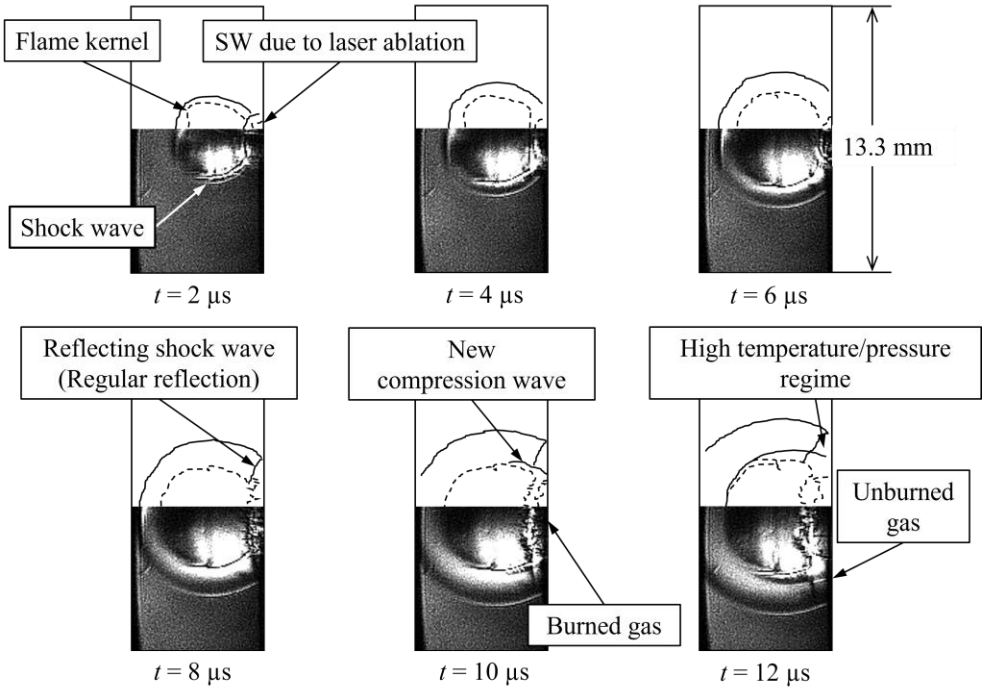

Figure 2: Schlieren images of the flow field (L = 3.66 mm) with a vertical reflection wall.

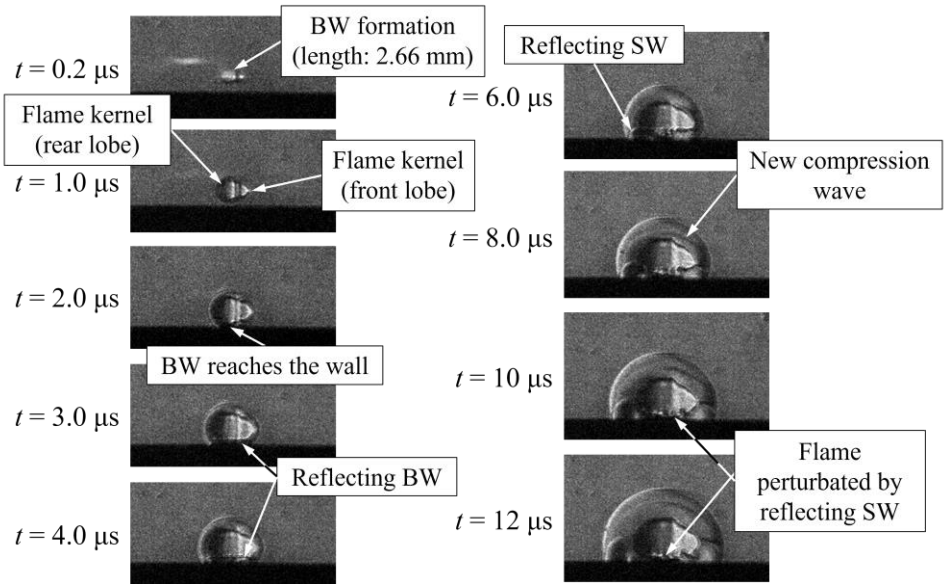

Figure 3: Schlieren images of the flowfield (L = 2.44 mm) with a horizontal reflection wall.

reflection was observed at t = 8 μs. As described in the sketch, high temperature/pressure region was observed behind the reflected blast wave at t =12 μs. Figure 3 shows the flowfield in the case of a horizontal reflection wall where the distance from the focal point to the wall was 2.44 mm. As observed in Figure 2, the generation and expansion, and a regular reflection of a blast wave were observed.

As observed in Figures 2 and 3, detonation was not initiated after blast wave reflection. Thus, the potential to initiate detonation is to be estimated based on the maximum pressure of the region behind the reflected blast wave in the case of the vertical reflection wall. Assuming that regular reflection occurred at the reflection point and that the curvature of the blast waves by the wall can be neglected as defined in Figure 4, maximum pressure p^* and maximum temperature T^* were calculated based on the Mach number of the reflection point and the following equations:

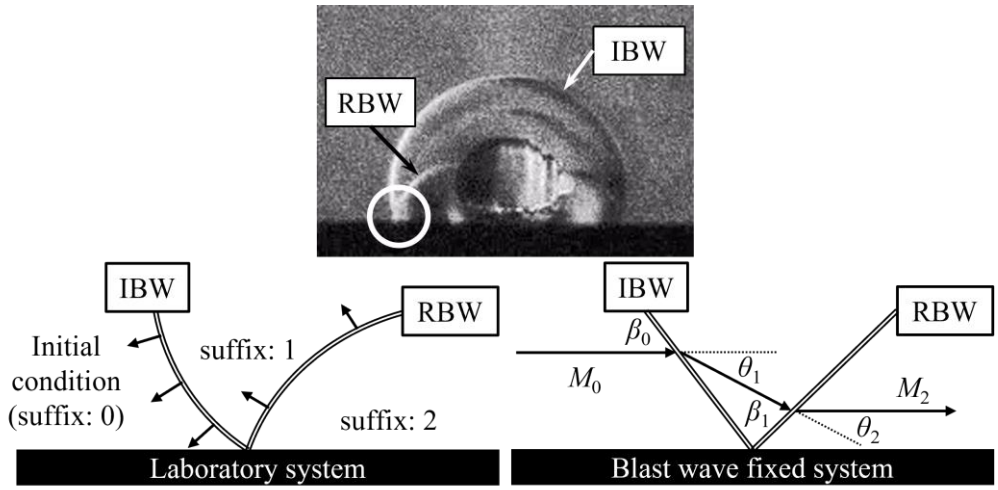

Figure 4: Definitions of the initial blast wave (IBW) and reflected blast wave (RBW) (top), and variables in the laboratory system (bottom left) and in the blast fixed system (bottom right).

$$\frac{p_{\mathrm{i}+1}}{p_{\mathrm{i}}} = 1 + \frac{2\gamma}{\gamma+1}\left(M_{\mathrm{i}}^2 \sin^2\beta_{\mathrm{i}} - 1\right) \tag{1}$$

$$\frac{T_{\mathrm{i}+1}}{T_{\mathrm{i}}} = \frac{\left(2\gamma M_{\mathrm{i}}^2 \sin^2\beta_{\mathrm{i}} - \gamma + 1\right)\left[(\gamma-1)M_{\mathrm{i}}^2 \sin^2\beta_{\mathrm{i}} + 2\right]}{(\gamma+1)^2 M_{\mathrm{i}}^2 \sin^2\beta_{\mathrm{i}}} \tag{2}$$

$$\tan\theta_{\mathrm{i}+1} = \frac{2\cot\beta_{\mathrm{i}}\left(M_{\mathrm{i}}^2 \sin^2\beta_{\mathrm{i}} - 1\right)}{M_{\mathrm{i}}^2(\gamma + \cos 2\beta_{\mathrm{i}}) + 2} \tag{3}$$

where M indicates the Mach number of the blast wave which is treated to be equal to the Mach number of the reflection point, θ indicates the angle of the blast wave, and ϕ indicates its deflection angle. The suffix i indicates the region of 0: initial condition, 1: behind the initial blast wave, and 2: behind the reflected blast wave. Figure 5 shows the comparisons of pressure, p^*, and temperature, T^*, at various focal point – reflection wall distances. As described in the figures, the maximum pressure almost follows a linear relationship and satisfies the mild ignition limit proposed by Meyer and Oppenheim [8]. Though the initiation of detonation waves was not recorded in any shots of experiments, it is implied that explosive reactions can occur after the reaction induction time in the high pressure/temperature region.

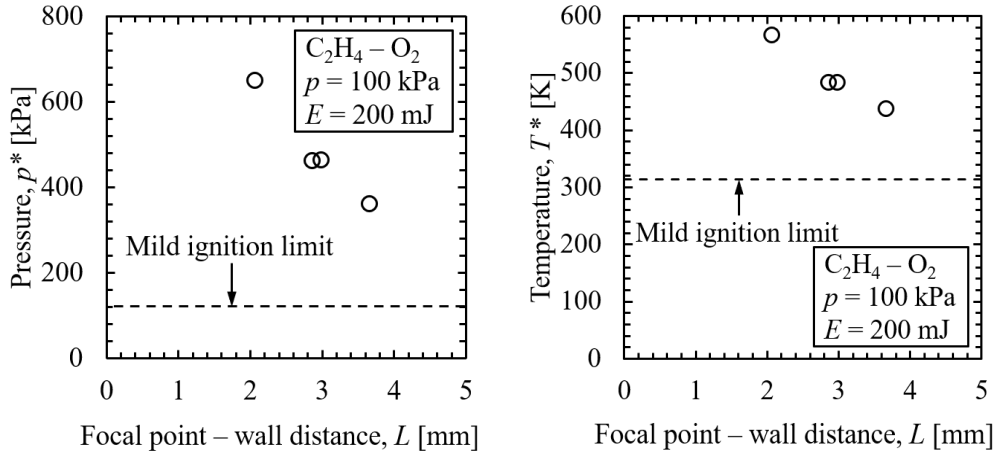

Fig. 5: Comparisons of maximum pressure (left) and maximum temperature (right) .

3.2 Laser ignition using an elliptic cavity

Figure 6 shows the successive schlieren images and their sketches of the flowfield after laser emission using an elliptic cavity. As well as in Figures 2 and 3, a spherical blast wave and a flame kernel were observed at t = 0.5 μs. At t = 1.5 μs, the blast wave touches the cavity wall, and two reflected blast waves can be observed at t = 2.5 μs. These reflected blast waves collide at the left end of the cavity and make a shock–shock intersection at laser time.

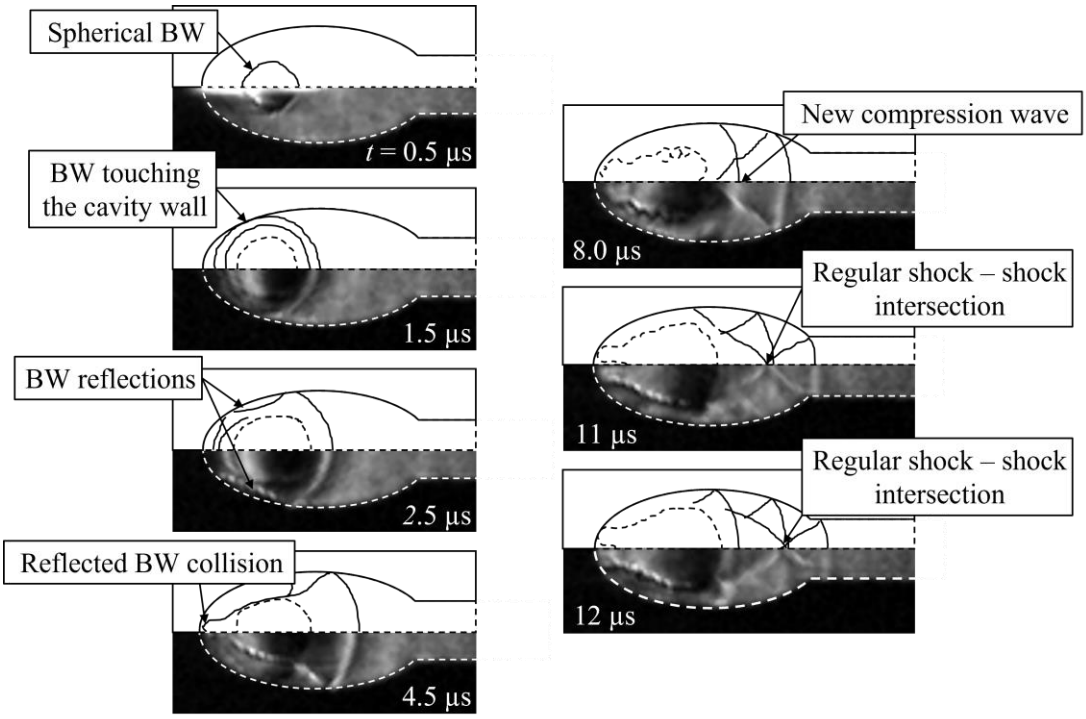

Figure 6: Schlieren images of the flow field after laser emission using an elliptic cavity. The laser comes from the left to the right side.

As the maximum pressure appears right after the shock–shock intersection, the pressure profile along the major axis of the ellipsoid was calculated based on the theory of regular shock–shock intersection. The variables and the suffixes before and after the intersection are defined in Figure 7, and the maximum pressure was calculated by Equations (1) and (3). Figure 8 shows the maximum pressure profile along the major axis of the elliptic cavity. The pressure reaches its peak at x = 0.977 where two reflected blast waves collide at the left end of the cavity and a shock-shock intersection occurs. The maximum pressure decays as the Mach number of the initial blast wave decreases which is an opposite profile calculated in previous studies about shock focusing [9]. This is due to the displacement of the laser beam's focusing point and the cavity's geometrical focal point. Due to this displacement, as observed in Figure 6, the initial blast wave reaches the cavity's walls at two points before reaching the endpoint of the cavity resulting in two convex reflection waves, not a single concave reflection wave.

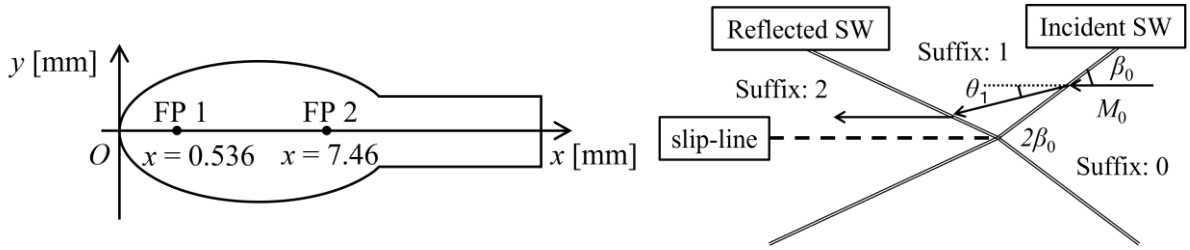

Figure 7: Definitions of x and y axis (left), suffixes, and variables (right) before and after the shock – shock intersection.

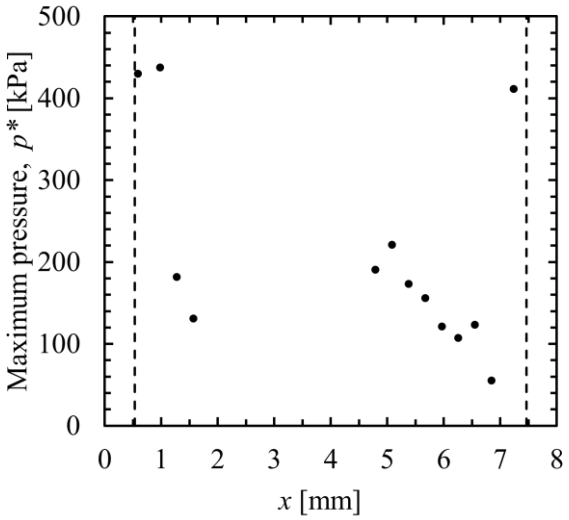

Figure 8: Maximum pressure profile along the major axis ($y = 0$) of the elliptic cavity.

4 Conclusions

Laser ignitions were conducted with two reflection walls and an elliptic cavity. As for the case of reflection walls, it was clarified that the high pressure/temperature region after reflected blast waves satisfies the mild ignition limit. Expansion waves behind the leading and reflected blast waves are considered to lower the unburned gas pressure resulting in longer ignition delay time. As for the elliptic cavity, blast wave reflections and shock–shock interaction was observed. From the pressure profile after the intersection, it was clarified that the displacement of the ignition point resulted in the difference between the reflected blast wave's propagation form and the displacement of the pressure peak.

References

[1] Wolański, P., "Detonative propulsion," *Proc. Comb. Institute,* Vol. 34, No. 1, 2013, pp. 125-158.

[2] Zeldovich, Y. B., "On the theory of the propagation of detonation in gaseous systems," *Zh. Eksp. Teor. Fiz.,* Vol. 10, No. 5, 1950, pp. 542-568.

[3] Nicholls, J. A ., Wilkinson, H. R. and Morrison, R. B., "Intermittent detonation as a thrust-producing mechanism," *Journal of jet prop.,* Vol. 27, No. 5, 1957, pp. 534-541.

[4] Nettleton, M. A., "Gaseous detonations: their nature, effects and control," *Springer Science & Business Media,* 2012.

[5] Urtiew, P. A. and Oppenheim, A. K., "Experimental observations of the transition to detonation in an explosive gas," *Proc. Royal Soc. London Series A,* Vol. 295, No. 1440, 1966, pp. 13-28.

[6] Lee, J. H. and Matsui, H., "A comparison of the critical energies for direct initiation of spherical detonations in acetylene – oxygen mixtures," *Comb. Flame,* Vol. 28, 1977, pp. 61-66.

[7] Bach, G. G., Knystautas, R., and Lee, J. H., "Direct initiation of spherical detonation in gaseous explosives," *12th Symp. (Int'l.) Comb.,* 1969, pp. 853-864.

[8] Meyer, J. W. and Oppenheim, A. K., "On the shock-induced ignition of explosive gases," *Symp. (Int'l.) Comb.,* Vol. 13, No. 1, pp. 1153-1164, 1971.

[9] Sturtevant, B. and Kulkarny, V. A., "The focusing of weak shock waves," *Journal of Fluid Mech.,* Vol. 73, No. 4, 1976, pp. 651-671.